Progress In Electromagnetics Research M, Vol. 70, 117–126, 2018

Study on the Vibration Mechanism of the Relay Coil in a Three-Coil WPT System

Suqi Liu[1, 2, *] and Jianping Tan[1, 2]

Abstract—Wireless power transfer (WPT) via coupled magnetic resonances has been in development for over a decade. Frequency splitting occurs in the over-coupled region. In addition, the vibration of the receiver and relay coils is observed in the over-coupled region. The vibration mechanism of the relay coil is investigated in this study. First, the circuit model of a three-coil WPT system is established, and the transfer characteristics of the system are examined by applying circuit theories. Second, the transfer characteristics of the three-coil WPT system are analyzed using simulation software. Third, the energy equation of state of the three-coil WPT system is established with the introduction of entropy variable. Lastly, the experimental circuit of the three-coil WPT system is designed. The experimental results are consistent with the theoretical analysis. The vibration of the relay coil is clearly explained. The transfer characteristics of the three-coil WPT system, particularly the relay coil, may provide ideas to achieve the maximum output power and transmission efficiency under various operating conditions.

1. INTRODUCTION

The theory of wireless power transfer has been developed since Nikola Tesla [1] demonstrated the principles of the WPT experiment more than 100 years ago. However, Tesla's prototype exhibited low efficiency, and its safety was uncertain. Electromagnetic radiation has been widely used for the wireless transmission of information. Magnetic induction and microwaves have been used for the transmission of power over distance in many applications. Inductive power transfer [2–4] has become a viable option for shorter distances because it has high-power transmission efficiency. In 2006, a research team of the Massachusetts Institute of Technology found that efficient mid-range WPT could be achieved using near-field magnetic coupling between two identical resonators [5]. Only when the coils are tuned to a particular resonance frequency can the coils transmit electricity through the air and around an obstacle with an acceptable level of efficiency. WPT has replaced conventional conductive battery chargers and has even been used to charge various portable consumer electronic, medical, and industrial devices [6–8].

As previously demonstrated, magnetically coupled resonators used for WPT have shown potential to deliver power with greater efficiency than that those of far-field approaches and at longer ranges than those of traditional inductively coupled schemes. However, in the over-coupled region, when the conditions for the maximum power theorem cannot be met at the resonance frequency of the resonators, frequency splitting occurs in mid-range WPT systems [9–11]. Thus, the output power of the two-coil system achieves the maximum output power at the two splitting angular frequencies and not at the resonance angular frequency [9]. By contrast, the transmission efficiency of the two-coil system achieves the maximum values at the resonance angular frequency and not at the two splitting angular frequencies. Beyond that, in the over-coupled region, the vibration of the receiver and that of the relay coils occur in the three-coil WPT system [12].

Received 26 April 2018, Accepted 28 June 2018, Scheduled 12 July 2018

* Corresponding author: Suqi Liu (liusuqi2009@126.com).

[1] Key Laboratory of High Performance Complex Manufacturing, Central South University, Changsha 410083, China. [2] School of Mechanical and Electrical Engineering, Central South University, Changsha 410083, China.

Ref. [12] mainly focuses on the modeling of the mechanism for the WPT system and explaining vibration. With the introduction of entropy [13, 14] the variable S, the energy equation of state can be established from the energies of the transmitter and receiver sides. According to the energy equation of state, two equations are obtained when the reactance of the transmitter and receiver sides equate zero. The vibration of the receiver coil in the three-coil WPT system was predicted and explained. In this study, the vibration mechanism of the relay coil was investigated, and the transfer characteristics of the three-coil WPT system, particularly the relay coil, were mined. First, the circuit model of the three-coil WPT system was established and the transfer characteristics of the system were examined by applying circuit theories. Second, the transfer characteristics of the three-coil WPT system were analyzed using simulation software. Third, the energy equation of state of the three-coil WPT system is established with the introduction of the entropy variable. Lastly, the experimental circuit of the three-coil WPT system was designed. The experimental results were consistent with the theoretical analysis; the vibration of the relay coil was well explained, and the transfer characteristics of the three-coil WPT system, particularly the relay coil, might provide ideas to achieve the maximum output power and transmission efficiency under various operating conditions.

2. MODELING OF THE THREE-COIL WPT SYSTEM

Figure 1 shows a diagram of the model of the three-coil WPT system. Figure 1(a) shows the sketch of the three-coil WPT system that includes the transmitter, relay, and receiver. The equivalent circuit model of the three-coil WPT system was then obtained, as shown in Figure 1(b).

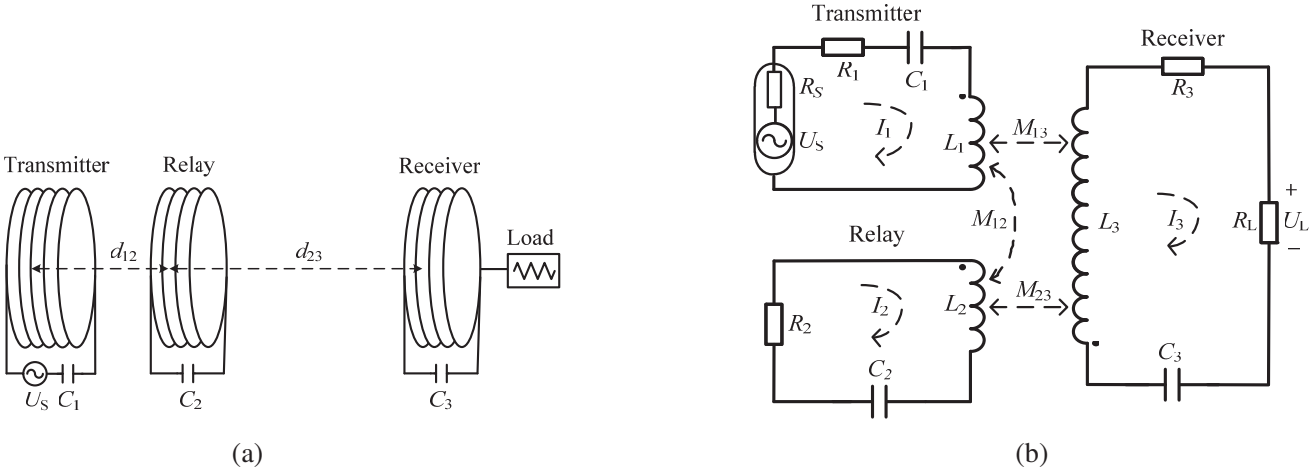

Figure 1. Model of the three-coil WPT system. (a) Sketch of the three-coil WPT system, including the transmitter, relay, and receiver; (b) Equivalent circuit model of the three-coil WPT system.

The equivalent circuit model consists of three resonant circuits, where U_S is the input power of the transmitter; R_S is the resistance of the U_S; R_1, R_2, and R_3 are the resistances of the coils; L_1, L_2, and L_3 are the inductances; C_1, C_2, and C_3 are the capacitances; R_L is the load resistance; and U_L is the load voltage. M_{12} is the mutual inductance between the transmitter and relay coils; M_{23} is the mutual inductance between the relay and receiver coils; and M_{13} is the mutual inductance between the transmitter and receiver coils. d_{12} is the coupling distance of the transmitter and relay coils, d_{23} is the coupling distance of the relay and receiver coils, and $d_{13} = d_{12} + d_{23}$ is the coupling distance of the transmitter and receiver coils.

This equivalent circuit model provides a convenient reference for the analysis of transfer characteristics of the WPT system. For simplicity, the assumed parameters of the transmitter, relay, and receiver are listed in Table 1.

Figure 1 shows the equivalent circuit model of the three-coil WPT system with a driving source of angular frequency ω, where Kirchhoff's voltage law is applied to determine the currents in each resonant

Table 1. Assumed values for the individual circuit elements of the transmitter, relay, and receiver.

Parameter	Value
Capacitances of the transmitter, relay and receiver	$C_1 = C_2 = C_3 = C$
Inductances of the transmitter, relay and receiver	$L_1 = L_2 = L_3 = L$
Resistance of the receiver	$R_3 + R_L = R$
Ratio of resistance of the load	$R_L = \beta R$
Ratio of resistance of the transmitter and receiver	$R_S + R_1 = \sigma_1 R(\sigma_1 > 0)$
Ratio of resistance of the relay and receiver	$R_2 = \sigma_2 R(\sigma_2 > 0)$
Resonance angular frequency of the system	$\omega_0 = 1/(LC)^{0.5}$
Resonance frequency of the system	$f_0 = \omega_0/2\pi$
Quality factor of the system	$Q_0 = \omega_0 L/R = 1/(\omega_0 CR)$
Frequency detuning factor of the system	$\xi = Q_0(\omega/\omega_0 - \omega_0/\omega)$
Resonance angular frequency of the transmitter, relay, and receiver	ω_0
Quality factor of the transmitter	$Q_1 = \omega_0 L/(R_S + R_1) = 1/(\omega_0 C(R_S + R_1)) = Q_0/\sigma_1$
Quality factor of the relay	$Q_2 = \omega_0 L/R_2 = 1/(\omega_0 CR_2) = Q_0/\sigma_2$
Quality factor of the receiver	$Q_3 = \omega_0 L/(R_3 + R_L) = 1/(\omega_0 C(R_3 + R_L)) = Q_0$

circuit in Equation (1), where I_1, I_2, and I_3 are the currents of the coils, and the self-impedance of the transmitter, relay, and receiver are defined in Equation (2).

$$\begin{cases} Z_1 I_1 + j\omega M_{12} I_2 + j\omega M_{13} I_3 = U_S \\ Z_2 I_2 + j\omega M_{12} I_1 + j\omega M_{23} I_3 = 0 \\ Z_3 I_3 + j\omega M_{13} I_1 + j\omega M_{23} I_2 = 0 \end{cases} \tag{1}$$

$$\begin{cases} Z_1 = R_S + R_1 + j\omega L_1 + \frac{1}{j\omega C_1} = R\left(\sigma_1 + \sigma_1 \frac{j\omega_0 L}{\sigma_1 R}\frac{\omega}{\omega_0} + \sigma_1 \frac{1}{j\sigma_1 R\omega_0 C}\frac{\omega_0}{\omega}\right) = R(\sigma_1 + j\xi) \\ Z_2 = R_2 + j\omega L_2 + \frac{1}{j\omega C_2} = R\left(\sigma_2 + \sigma_2 \frac{j\omega_0 L}{\sigma_2 R}\frac{\omega}{\omega_0} + \sigma_2 \frac{1}{j\sigma_2 R\omega_0 C}\frac{\omega_0}{\omega}\right) = R(\sigma_2 + j\xi) \\ Z_3 = R_3 + R_L + j\omega L_3 + \frac{1}{j\omega C_3} = R\left(1 + \frac{j\omega_0 L}{R}\frac{\omega}{\omega_0} + \frac{1}{jR\omega_0 C}\frac{\omega_0}{\omega}\right) = R(1 + j\xi) \end{cases} \tag{2}$$

According to [12], $(\omega M)^2/Z_{11}$ and $(\omega M)^2/Z_{22}$ represent the reflecting impedances. For convenience of analysis, the impedance coupling factors τ_{12}, τ_{23}, and τ_{13} are defined in Equation (3), which indicates the ability of impedance coupling, where M is the mutual inductance of the transmitter and receiver coils, $Z_{11} = R_1 + R_S + j\omega L_1 + 1/(j\omega C_1)$, and $Z_{22} = R_2 + R_L + j\omega L_2 + 1/(j\omega C_2)$.

$$\begin{cases} \tau_{12} = \frac{\omega M_{12}}{\sqrt{R_1 R_2}} = \frac{\omega M_{12}}{\sqrt{\sigma_1\sigma_2}R}, & \tau_{12} > 0 \\ \tau_{23} = \frac{\omega M_{23}}{\sqrt{R_2(R_3+R_L)}} = \frac{\omega M_{23}}{\sqrt{\sigma_2}R}, & \tau_{23} > 0 \\ \tau_{13} = \frac{\omega M_{13}}{\sqrt{R_1(R_3+R_L)}} = \frac{\omega M_{13}}{\sqrt{\sigma_1}R}, & \tau_{13} > 0 \end{cases} \tag{3}$$

According to Equations (1), (2), and (3), as well as the definitions in Table 1, the currents of the transmitter, relay, and receiver coils can be written as

$$\begin{cases} I_1 = \frac{(1+j\xi)(\sigma_2+j\xi)+\sigma_2\tau_{23}^2}{(1+j\xi)(\sigma_1+j\xi)(\sigma_2+j\xi)+\sigma_1\sigma_2(1+j\xi)\tau_{12}^2+\sigma_2(\sigma_1+j\xi)\tau_{23}^2+\sigma_1(\sigma_2+j\xi)\tau_{13}^2-j2\sigma_1\sigma_2\tau_{12}\tau_{23}\tau_{13}}\frac{U_S}{R} \\ I_2 = \frac{(\xi-j)\sqrt{\sigma_1\sigma_2}\tau_{12}-\sqrt{\sigma_1\sigma_2}\tau_{23}\tau_{13}}{(1+j\xi)(\sigma_1+j\xi)(\sigma_2+j\xi)+\sigma_1\sigma_2(1+j\xi)\tau_{12}^2+\sigma_2(\sigma_1+j\xi)\tau_{23}^2+\sigma_1(\sigma_2+j\xi)\tau_{13}^2-j2\sigma_1\sigma_2\tau_{12}\tau_{23}\tau_{13}}\frac{U_S}{R} \\ I_3 = \frac{(\xi-j\sigma_2)\sqrt{\sigma_1}\tau_{13}-\sqrt{\sigma_1}\sigma_2\tau_{12}\tau_{23}}{(1+j\xi)(\sigma_1+j\xi)(\sigma_2+j\xi)+\sigma_1\sigma_2(1+j\xi)\tau_{12}^2+\sigma_2(\sigma_1+j\xi)\tau_{23}^2+\sigma_1(\sigma_2+j\xi)\tau_{13}^2-j2\sigma_1\sigma_2\tau_{12}\tau_{23}\tau_{13}}\frac{U_S}{R} \end{cases} \tag{4}$$

According to the root mean square (RMS) current I_2 of the relay coil, the power of the relay side is $P_{\text{relay}} = |I_2|^2 R_2$. If $\tau_{12} = 1$, $\tau_{23} = \tau_{13} = 0$, and $\xi = 0$, the maximum power of the relay is

$P_{\text{relay max}} = U_S^2/(4\sigma_1 R)$. Thus, the normalized power of the relay is

$$\begin{aligned}\psi_{\text{relay}} &= \frac{P_{\text{relay}}}{P_{\text{relay max}}} \\ &= \frac{4\sigma_1^2\sigma_2^2\left[\tau_{12}^2 + (\tau_{23}\tau_{13} - \xi\tau_{12})^2\right]}{\left\{\begin{array}{c}\left[\sigma_1\sigma_2(1+\tau_{12}^2+\tau_{23}^2+\tau_{13}^2) - (1+\sigma_1+\sigma_2)\xi^2\right]^2 \\ +\left[\xi\left(\sigma_1+\sigma_2+\sigma_1\sigma_2+\sigma_1\sigma_2\tau_{12}^2+\sigma_2\tau_{23}^2+\sigma_1\tau_{13}^2-\xi^2\right) - 2\sigma_1\sigma_2\tau_{12}\tau_{23}\tau_{13}\right]^2\end{array}\right\}}\end{aligned} \tag{5}$$

According to the RMS I_3 of the receiver-coil, the power of the receiver side is $P_{out} = |I_3|^2 R_L$. If $\tau_{13} = 1$, $\tau_{12} = \tau_{23} = 0$, and $\xi = 0$, the maximum power of the receiver is $P_{out\,\max} = \beta U_S^2/(4\sigma_1 R)$. Thus, the normalized power of the receiver can be expressed as

$$\begin{aligned}\psi_{out} &= \frac{P_{out}}{P_{out\,\max}} \\ &= \frac{4\sigma_1^2\left[(\sigma_2\tau_{12}\tau_{23} - \xi\tau_{13})^2 + (\sigma_2\tau_{13})^2\right]}{\left\{\begin{array}{c}\left[\sigma_1\sigma_2(1+\tau_{12}^2+\tau_{23}^2+\tau_{13}^2) - (1+\sigma_1+\sigma_2)\xi^2\right]^2 \\ +\left[\xi(\sigma_1+\sigma_2+\sigma_1\sigma_2+\sigma_1\sigma_2\tau_{12}^2+\sigma_2\tau_{23}^2+\sigma_1\tau_{13}^2-\xi^2) - 2\sigma_1\sigma_2\tau_{12}\tau_{23}\tau_{13}\right]^2\end{array}\right\}}\end{aligned} \tag{6}$$

The transmission efficiency of the relay is given by

$$\begin{aligned}\eta_{\text{relay}} &= \frac{P_{rel}}{P_{in}} = \frac{|I_2|^2 R_2}{|I_1|^2(R_S+R_1) + |I_2|^2 R_2 + |I_3|^2(R_3+R_L)} \\ &= \frac{\sigma_2^2\left[(\tau_{23}\tau_{13} - \xi\tau_{12})^2 + \tau_{12}^2\right]}{(\sigma_2+\sigma_2\tau_{23}^2-\xi^2)^2 + (1+\sigma_2)^2\xi^2 + \sigma_2^2\left[(\tau_{23}\tau_{13}-\xi\tau_{12})^2+\tau_{12}^2\right] + (\sigma_2\tau_{12}\tau_{23}-\xi\tau_{13})^2 + (\sigma_2\tau_{13})^2}\end{aligned} \tag{7}$$

The transmission efficiency of the receiver is given by

$$\begin{aligned}\eta_{out} &= \frac{P_{out}}{P_{in}} = \frac{|I_3|^2 R_L}{|I_1|^2(R_S+R_1) + |I_2|^2 R_2 + |I_3|^2(R_3+R_L)} \\ &= \frac{\beta\left[(\sigma_2\tau_{12}\tau_{23} - \xi\tau_{13})^2 + (\sigma_2\tau_{13})^2\right]}{(\sigma_2+\sigma_2\tau_{23}^2-\xi^2)^2 + (1+\sigma_2)^2\xi^2 + \sigma_2^2\left[(\tau_{23}\tau_{13}-\xi\tau_{12})^2+\tau_{12}^2\right] + (\sigma_2\tau_{12}\tau_{23}-\xi\tau_{13})^2 + (\sigma_2\tau_{13})^2}\end{aligned} \tag{8}$$

3. SIMULATION OF TRANSFER CHARACTERISTICS

According to Equations (5) and (6), given $\sigma_1 = 1$, $\sigma_2 = 0.1$, and $\tau_{12} = 4$, the normalized power of the relay is as plotted in Figure 2(a), and the normalized power of the receiver is as plotted in Figure 2(b). The normalized powers of the relay and receiver depend on parameters ξ, σ_1, σ_2, τ_{12}, τ_{23}, and τ_{13}. In Figure 2(a), the normalized power of the relay shows two peaks, which indicate the occurrence of frequency splitting. According to the frequency detuning factor $\xi = Q_0(\omega/\omega_0 - \omega_0/\omega)$, the relay achieves the maximum output power at the two splitting angular frequencies ω_1 and ω_2, which belong to a lower frequency mode and a higher frequency mode, respectively. In addition, the function of the relay is mainly to transfer the power from the transmitter to the receiver but not to consume the power. In Figure 2(b), the normalized power of the receiver also shows two peaks. Owing to the effect of the impedance coupling factor τ_{13} on the three-coil WPT system, the width of the power peak of the higher frequency mode is larger than that of the lower frequency mode.

According to Equations (7) and (8), given $\sigma_1 = 1$, $\sigma_2 = 0.1$, and $\tau_{12} = 4$, the transmission efficiency of the relay is as plotted in Figure 3(a); the transmission efficiency of the receiver is as plotted in Figure 3(b). The transmission efficiencies of the relay and receiver depend on parameters ξ, σ_1, σ_2, τ_{12}, τ_{23}, and τ_{13}. In Figure 3(a), the transmission efficiency of the relay shows two peaks. The transmission efficiency of the relay is considerably low because the relay transfers but not consumes the power. In Figure 3(b), owing to the effect of the impedance coupling factor τ_{13} on the three-coil WPT system, the transmission efficiency of the receiver has only one peak; the peaks move toward the lower-frequency direction.

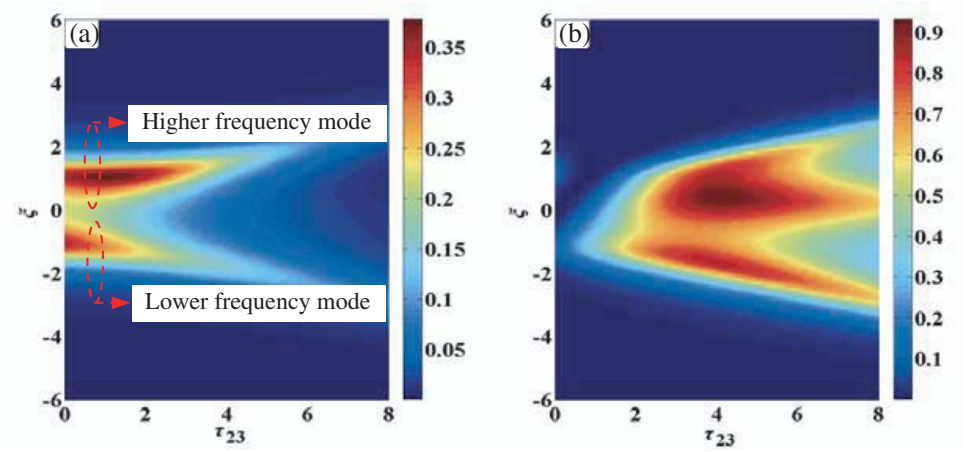

Figure 2. Characteristic curves of the normalized output power of the system. (a) Characteristic curves of the normalized power of the relay ψ_{relay}; (b) Characteristic curves of the normalized power of the receiver ψ_{out}. (a) $\sigma_1 = 1$, $\sigma_2 = 0.1$, $\tau_{12} = 4$, (b) $\sigma_1 = 1$, $\sigma_2 = 0.1$, $\tau_{12} = 4$.

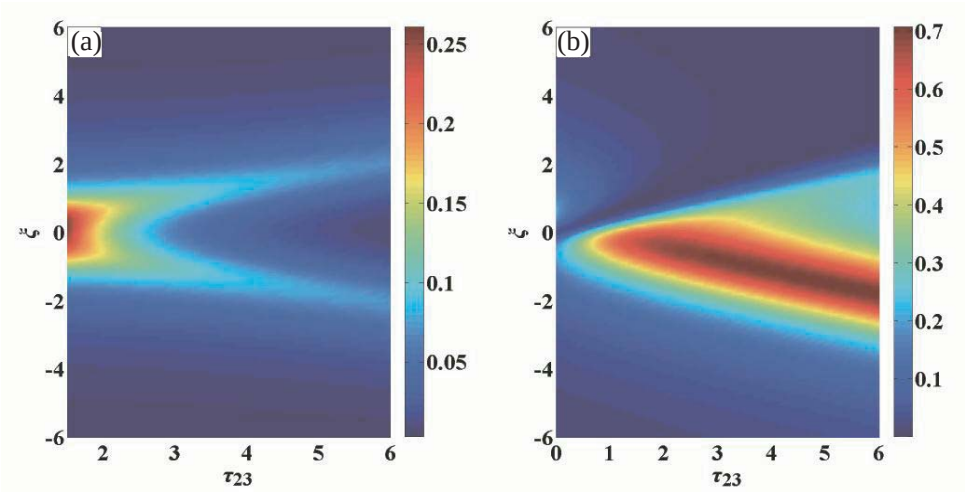

Figure 3. Characteristic curves of the transmission efficiency of the system. (a) Characteristic curves of the transmission efficiency of the relay η_{relay} when $\beta = 1$; (b) Characteristic curves of the transmission efficiency of the receiver η_{out} when $\beta = 1$. (a) $\sigma_1 = 1$, $\sigma_2 = 0.1$, $\tau_{12} = 4$, (b) $\sigma_1 = 1$, $\sigma_2 = 0.1$, $\tau_{12} = 4$.

4. SELF-ORGANIZATION THEORY AND EQUATION OF ENERGY ENTROPY

Self-organization [15, 16] is a process where some form of overall order arises from local interactions between parts of an initially disordered system. The process is spontaneous, not needing control by any external agent. It is often triggered by random fluctuations and amplified by positive feedback. The resulting organization is wholly decentralized. Self-organization occurs in many physical, chemical, biological, robotic, and cognitive systems. Examples can be found in crystallization, thermal convection of fluids, chemical oscillation, and so on.

When a three-coil WPT system uses the ZCS technique, it uses four criteria to evaluate whether a WPT system obeys the self-organization theory: (1) Openness. Continuous energy supply allows the WPT system to exchange energy with the outside system. For example, the WPT system absorbs the energies from the voltage source and the energies are consumed by loads; (2) Fluctuation and mutation. There is one power peak in the under-coupled region and the critically-coupled point. When the coupling distance decreases, the system moves into the over-coupled region and shows two power

peaks; that is, the WPT system achieves the maximum output power at the two splitting angular frequencies and not at the resonance angular frequency; (3) Nonlinearity. In the over-coupled region, the WPT system obtains a nonlinear equation when the system energy equation of state was created and further, the maximum value of the output power was obtained; that is, the nonlinear equation $\sigma_1 + \sigma_2 + \sigma_1\sigma_2 + \sigma_1\sigma_2\tau_{12}^2 + \sigma_2\tau_{23}^2 + \sigma_1\tau_{13}^2 - \xi^2 = 0$ was obtained from Equations (5), (6), and (9); (4) Far from equilibrium. In the over-coupled region, the output power of the WPT system achieves the maximum output power at the two splitting frequencies and not at the natural resonant frequency. Thus, the three-coil WPT system is a self-organizing system.

Rudolf Julius Emanuel Clausius is considered one of the central founders of the science of thermodynamics. By his restatement of Sadi Carnot's principle known as the Carnot cycle, he gave the theory of heat a truer and sounder basis. His most important paper, "On the Moving Force of Heat," which was published in 1850, first stated the basic ideas of the second law of thermodynamics. In 1865, he introduced the concept of entropy [17]. Although the concept of entropy was originally a thermodynamic construct, it has been adapted in other fields of study, including information theory [18], ecological economics [19], evolution [20], and so on. With the introduction of the entropy variable S, the energy equation of state can be established based on the energies of the transmitter, relay, and receiver sides. The expression can be given as

$$\begin{aligned}
\frac{dS}{dt} &= (P_{I1} + P_{I2} + P_{I3}) - (P_{A1} + P_{A2} + P_{A3}) \\
&= \left(|I_1|^2 X_1 + |I_2|^2 X_2 + |I_3|^2 X_3\right) - \left(|I_1|^2 R_1 + |I_2|^2 R_2 + |I_3|^2 R_3\right) \\
&= \left\{ \xi \frac{\left[(\sigma_2+\sigma_2\tau_{23}^2-\xi^2)^2+(\xi+\sigma_2\xi)^2\right]+\sigma_1\sigma_2\left[\tau_{12}^2+(\tau_{23}\tau_{13}-\xi\tau_{12})^2\right]+\sigma_1\left[(\sigma_2\tau_{12}\tau_{23}-\xi\tau_{13})^2+(\sigma_2\tau_{13})^2\right]}{\left\{ \begin{array}{c} \left[\sigma_1\sigma_2(1+\tau_{12}^2+\tau_{23}^2+\tau_{13}^2)-(1+\sigma_1+\sigma_2)\xi^2\right]^2 \\ +\left[\xi(\sigma_1+\sigma_2+\sigma_1\sigma_2+\sigma_1\sigma_2\tau_{12}^2+\sigma_2\tau_{23}^2+\sigma_1\tau_{13}^2-\xi^2)-2\sigma_1\sigma_2\tau_{12}\tau_{23}\tau_{13}\right]^2 \end{array} \right\}} \right. \\
&\quad \left. - \frac{\sigma_1\left[(\sigma_2+\sigma_2\tau_{23}^2-\xi^2)^2+(\xi+\sigma_2\xi)^2\right]+\sigma_1\sigma_2^2\left[\tau_{12}^2+(\tau_{23}\tau_{13}-\xi\tau_{12})^2\right]+\sigma_1\left[(\sigma_2\tau_{12}\tau_{23}-\xi\tau_{13})^2+(\sigma_2\tau_{13})^2\right]}{\left\{ \begin{array}{c} \left[\sigma_1\sigma_2(1+\tau_{12}^2+\tau_{23}^2+\tau_{13}^2)-(1+\sigma_1+\sigma_2)\xi^2\right]^2 \\ +\left[\xi(\sigma_1+\sigma_2+\sigma_1\sigma_2+\sigma_1\sigma_2\tau_{12}^2+\sigma_2\tau_{23}^2+\sigma_1\tau_{13}^2-\xi^2)-2\sigma_1\sigma_2\tau_{12}\tau_{23}\tau_{13}\right]^2 \end{array} \right\}} \right\} \frac{U_S^2}{R}
\end{aligned} \tag{9}$$

where S is the energy entropy [21, 22], which is a measure of disorder. High-energy entropy states are relatively disordered, whereas low-energy entropy states are relatively ordered. Let t be the time, and P_{I1}, P_{I2}, and P_{I3} be the imaginary powers of the transmitter, relay, and receiver, respectively, which are stored on the reactive loads; P_{A1}, P_{A2}, and P_{A3} be the active powers of the transmitter, relay, and receiver respectively, which are consumed on the resistive loads.

When a three-coil system operates in an over-coupled region [9, 12], the imaginary powers $P_{I1} + P_{I2} + P_{I3}$ should achieve the minimum value; that is, the system moves to a new stable state without any control by any external agent. According to Equation (9) and ignoring the higher term $2\sigma_1\sigma_2\tau_{12}\tau_{23}\tau_{13}$, the system has three roots: $\xi_1 = -(\sigma_1 + \sigma_2 + \sigma_1\sigma_2 + \sigma_1\sigma_2\tau_{12}^2 + \sigma_2\tau_{23}^2 + \sigma_1\tau_{13}^2)^{0.5}$, $\xi_2 = 0$, and $\xi_3 = (\sigma_1 + \sigma_2 + \sigma_1\sigma_2 + \sigma_1\sigma_2\tau_{12}^2 + \sigma_2\tau_{23}^2 + \sigma_1\tau_{13}^2)^{0.5}$ when the reactance of the three-coil WPT system equals zero.

5. EXPERIMENTAL RESULTS OF THE VIBRATION OF THE RELAY COIL

Figure 4 shows the three-coil experimental setup of the relay coil vibration; the system includes the wave generator, power amplifier, current probe, voltage probe, oscilloscope, capacitances, transmitter, relay, receiver, load, transmitter coil, relay coil, and receiver coil. The parameters of the transmitter, relay, and receiver are listed in Table 2.

According to ξ_1, ξ_2, and ξ_3, the system obtains the three eigenfrequencies ω_1, ω_0, and ω_2, respectively. With the effect of the coupled factor τ_{13}, the three eigenfrequencies of the relay move

Table 2. Experimental parameters of the transmitter, relay, and receiver.

Parameter	Transmitter	Relay	Receiver
Frequency f_0/kHz	195	195	195
Inductance L/μH	29.25	29.25	29.25
Capacitance C/nF	22.77	22.77	22.77
Internal/external radius r/mm	15.0/19.0	15.0/19.0	15.0/19.0
Wire radius r/mm	0.5		
Material	copper		
Number of turns	20		
Impedance scaling factor σ_1	1		
Impedance scaling factor σ_2		0.1	
Load resistance R_L/Ω		4	

toward the higher-frequency direction, as shown in Figure 5(a). By contrast, the three eigenfrequencies of the receiver move toward the lower-frequency direction, as shown in Figure 5(b). Similarly, the curves of the transmission efficiency of the relay appear the two peaks; and the efficiency peaks of the relay move toward the higher-frequency direction, as shown in Figure 6(a). By contrast, the efficiency peaks

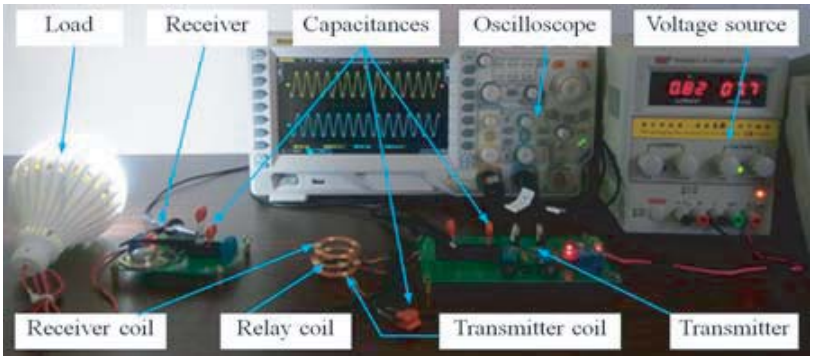

Figure 4. Vibrating experimental system of the relay coil.

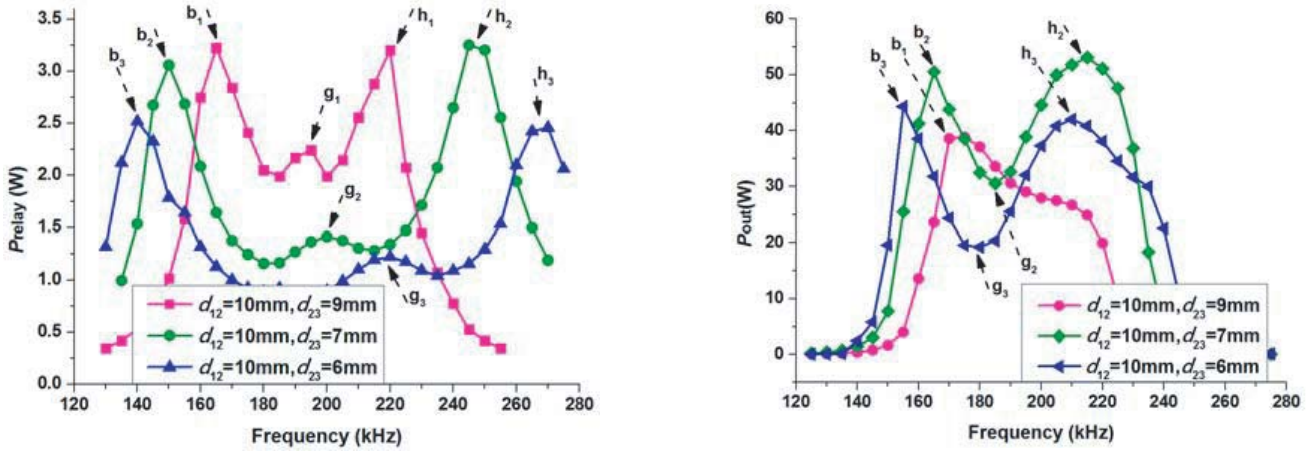

(a) (b)

Figure 5. Curves of the output power of the three-coil WPT system that includes the relay and the receiver. (a) Curves of the output power of the relay; (b) Curves of the output power of the receiver.

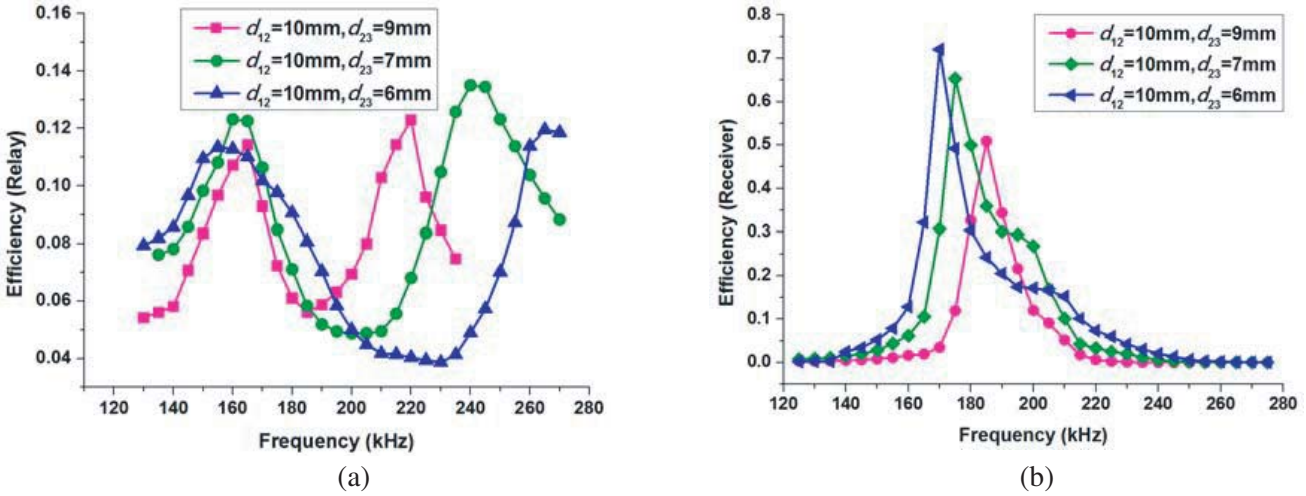

Figure 6. Curves of the transmission efficiency of the three-coil WPT system that includes the relay and the receiver. (a) Curves of the transmission efficiency of the relay; (b) Curves of the transmission efficiency of the receiver.

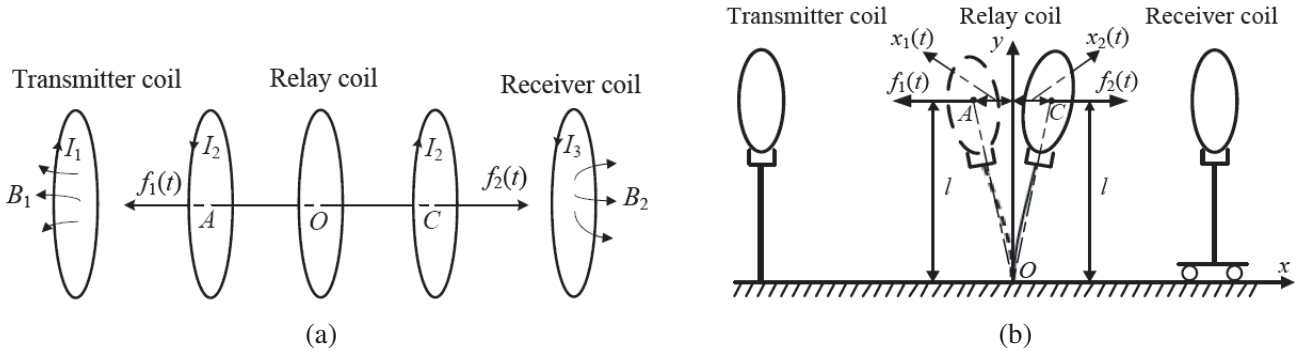

Figure 7. Force diagram of the three-coil WPT system. (a) Lorentz force of the relay coil; (b) Force diagram of the relay-coil.

of the receiver move toward the lower-frequency direction, as shown in Figure 6(b). The function of the relay is mainly to transfer power and not to consume power; thus, the transmission efficiency of the relay is considerably low. However, the function of the receiver is the opposite. In conclusion, the results of the experiment are consistent with the results of the simulation.

A relationship exists among the eigenfrequency points b, g, h and the angular frequencies ω_1, ω_0, ω_2, respectively. In accordance with the energy entropy theory, Figure 5(a) shows that the three-coil system stores the minimum imaginary power at points b_1, b_2, b_3, h_1, h_2, and h_3, which belong to the stable frequency point ω_1 or ω_2. By contrast, the three-coil system stores the maximum imaginary power at points g_1, g_2, and g_3, which belong to the unstable frequency point ω_0; that is, the system tend to move from the unstable frequency point to the stable frequency point without any control by an external agent. In Figure 5(a), in accordance with the current phase between the transmitter and relay coils, the currents of the transmitter and relay coils are in-phase at points b_1, b_2, and b_3; the currents are zero-phase at points g_1, g_2, and g_3; and the currents are anti-phase at points h_1, h_2, and h_3. The frequency and distance exhibit a one-to-one relationship; different distances between the two coils should be tuned to different frequencies. As shown in Figure 7, in accordance with the Lorentz force law [23], on the OA side, the electromagnetic force $f_1(t)$ tends to gradually increase until the relay coil achieves the maximum value at point A because the output power of the relay coil gradually increases

until the maximum output power is achieved at point b_1 (or b_2 or b_3); similarly, on the OC side, the electromagnetic force $f_2(t)$ tends to gradually increase until the relay coil achieves the maximum value at point C because the output power of the relay coil gradually increases until the maximum output power is achieved at point h_1 (or h_2, or h_3); point O is a critical point, the phase and electromagnetic force of the relay coil tends to be reversed subsequently. While the relay coil merely moves to point g_1 (g_2 or g_3) by adjusting the position of the receiver coil, stimulating the relay coil with artificial perturbation force can cause the relay coil to leave from point g_1 (g_2 or g_3). The relay coil generates forced vibration between point b_1 (b_2 or b_3) and point h_1 (h_2 or h_3), namely, at points A and C. As shown in Figures 5(a) and 6(a), the peaks of the output power of the receiver coil exhibit periodic variation, and the transmission efficiencies of the receiver coil exhibit periodic fluctuation because the periodic vibration of the relay coil occurs between the point b_1 (b_2 or b_3) and point h_1 (h_2 or h_3). The factors influencing the occurrence of vibration are further investigated.

Vibration is commonly known as a mechanical phenomenon whereby oscillations occur about an equilibrium point. Types of vibration include forced vibration, damped vibration, and so on. Forced vibration occurs when the object is forced to vibrate at a particular frequency via a periodic input of force. Thus, the vibration of the relay coil is a force vibration. In this study, the force analysis of the relay coil is given. In Figure 7(b), the relay coil can be regarded as a slender rod; the mass of the relay coil m may be concentrated in the geometric center of the relay coil; and the electromagnetic forces $f_1(t)$ or $f_2(t)$ acting on the relay coil are located at the geometric center. When a slender rod is perpendicular to the x axis, its deformation is the bending deformation of the beam. According to mechanical vibration [24], the free end of the beam will have disturbances of $x_1(t) = f_1(t)l^3/(3EJ))$ or $x_2(t) = f_2(t)l^3/(3EJ)$ under the action of electromagnetic forces $f_1(t)$ or $f_2(t)$. In this study, the cantilever beam acts as a spring, and the force required by the free end to produce unit deformation is the spring coefficient k of the beam. Under the excitation of electromagnetic forces $f_1(t)$ or $f_2(t)$, the relay coil is stimulated with an artificial perturbation force and leaves the central position Oy. The vibration system of a cantilever beam with single degree of freedom will be subjected to periodic steady-state vibration. The motion differential equations of the relay coil are given by

$$\begin{cases} m\ddot{x}_1(t) + kx_1(t) = f_1(t), & x < 0 \\ m\ddot{x}_2(t) + kx_2(t) = f_2(t), & x > 0 \end{cases} \tag{10}$$

where $x_1(t)$ or $x_2(t)$ are the lateral displacements of the beam, and k is the spring coefficient. In $k = 3EJ/l^3$, EJ is the bending stiffness, E is the elastic modulus, J is the moment of inertia, and l is the vertical distance between the geometric center of the relay coil and the x axis. A and C are the left and right extreme positions of the relay coil when the three-coil system operates in the vibrating state. B_1 and B_2 are the electromagnetic fields.

6. CONCLUSION

This study provides a deeper understanding of the underlying principles of coupled magnetic resonances by applying the self-organization theory and energy entropy theory. It shows that the WPT system belongs to a self-organizing system and investigates the vibration of the relay coil. The peaks of the output power of the receiver coil exhibit periodic variation because of the periodic vibration of the relay coil. The transmission efficiency of the receiver coil exhibits periodic fluctuation. The transfer characteristics of the three-coil WPT system, particularly the relay coil, may provide ideas to achieve the maximum output power and transmission efficiency under various operating conditions. For example, the output power and transmission efficiency of the receiver are affected by the relay coil, and an efficient topology of the WPT system may be proposed that the functions of the relay coil are transformed into functions of the compensator to compensate for the impedance of the system.

ACKNOWLEDGMENT

This work was supported by the National Key Basic Research Program of China (2014CB049405).

REFERENCES

1. Tesla, N., U.S. Patent, 1119732, 1914.
2. Schirmer, J. and H. Kazmierczak, U.S. Patent, 20040008036, 2004.
3. Kissin, M. L. G., J. T. Boys, and G. A. Covic, "Interphase mutual inductance in polyphase inductive power transfer systems," *IEEE Transactions on Industrial Electronics*, Vol. 56, No. 7, 2393, 2009.
4. Duong, Q. T. and M. Okada, "kQ-product formula for multiple-transmitter inductive power transfer system," *IEICE Electronics Express*, Vol. 14, 20161167, 2017.
5. Kurs, A., A. Karalis, R. Moffatt, J. D. Joannopoulos, P. Fisher, and M. Soljacic, "Wireless power transfer via strongly coupled magnetic resonances," *Science*, Vol. 317, No. 5834, 83, 2007.
6. Tamura, M., Y. Watanabe, and I. Takano, "Waveguide-mode wireless power transfer in shielded space with aperture plane," *IEICE Electronics Express*, Vol. 14, 20170195, 2017.
7. Takeno, K., "Wireless power transmission technology for mobile devices," *IEICE Electronics Express*, Vol. 10, 20132010, 2013.
8. Nguyen, V. T., S. H. Kang, J. H. Choi, et al., "Magnetic resonance wireless power transfer using three-coil system with single planar receiver for laptop applications," *IEEE Transactions on Consumer Electronics*, Vol. 61, No. 2, 160, 2015.
9. Sample, A. P., D. A. Meyer, and J. R. Smith, "Experimental results, and range adaptation of magnetically coupled resonators for wireless power transfer," *IEEE Transactions on Industrial Electronics*, Vol. 58, No. 2, 544, 2011.
10. Huang, R., B. Zhang, D. Qiu, et al., "Frequency splitting phenomena of magnetic resonant coupling wireless power transfer," *IEEE Transactions on Magnetics*, Vol. 50, No. 11, 1, 2014.
11. Liu, S., J. Tan, S. Xue, et al., "Analysis on coupling mechanism characteristics of multi-load wireless power transmission system," *Automation of Electric Power Systems*, Vol. 40, No. 18, 84, 2016.
12. Liu, S., J. Tan, and X. Wen, "Modeling of coupling mechanism of wireless power transfer system and vibration phenomenon of receiver-coil in three-coil system," *AIP Advances*, Vol. 7, 115107, 2017.
13. Deng, Z., W. Lin, N. Li, et al., "The uncertainty entropy of low-rate speech quality evaluation and the analyses of the gray correlation," *IEICE Electron Express*, Vol. 12, No. 3, 20141019, 2015.
14. Martyushev, L. M. and V. D. Seleznev, "The restrictions of the maximum entropy production principle," *Physica A Statistical Mechanics & Its Applications*, Vol. 410, No. 15, 17, 2014.
15. Ashby, W. R., "Principles of the self-organizing dynamic system," *The Journal of General Psychology*, Vol. 37, No. 2, 125, 1947.
16. Serugendo, G. Di Marzo, et al., "Self-organization in multi-agent systems," *Knowledge Engineering Review*, Vol. 20, No. 2, 165, 2006.
17. Baker, T., M. Asim, H. Tawfik, et al., "An energy-aware service composition algorithm for multiple cloud-based IoT applications," *Journal of Network & Computer Applications*, Vol. 89, 96, 2017.
18. Baker, T., B. Al-Dawsari, H. Tawfik, et al., "GreeDi: An energy efficient routing algorithm for big data on cloud," *Ad Hoc Networks*, Vol. 35, 83, 2015.
19. Hammond, G. P. and A. B. Winnett, "The influence of thermodynamic ideas on ecological economics: An interdisciplinary critique," *Sustainability*, Vol. 1, No. 4, 1195, 2009.
20. Chiavazzo, E., M. Fasano, and P. Asinari, "Inference of analytical thermodynamic models for biological networks," *Physica A: Statistical Mechanics and Its Applications*, Vol. 392, No. 5, 1122, 2013.
21. Entropy, https://en.wikipedia.org/wiki/Entropy.
22. Cropper, W. H., *Great Physicists: The Life and Times of Leading Physicists from Galileo to Hawking*, 93–105, Oxford University Press, London, United Kingdom, 2004, ISBN 978-0-19-517324-6.
23. Lorentz force, https://en.wikipedia.org/wiki/Lorentz_force.
24. Tse, F. S., I. E. Morse, and R. T. Hinckle, *Mechanical Vibrations: Theory and Applications*, 2nd Edition, 93, Allyn and Bacon, Boston, Massachusetts, 1978.